Scripta Materialia 114 (2016) 79–83

Contents lists available at ScienceDirect

Scripta Materialia

journal homepage: www.elsevier.com/locate/scriptamat

Real-time X-ray microscopy study of electromigration in microelectronic solder joints

Cheng-En Ho *, Cheng-Hsien Yang, Pei-Tzu Lee, Chih-Tsung Chen

Department of Chemical Engineering & Materials Science, Yuan Ze University, Chungli Dist., Taoyuan City 320, Taiwan, ROC

ARTICLE INFO

Article history:
Received 3 October 2015
Received in revised form 5 November 2015
Accepted 1 December 2015
Available online 17 December 2015

Keywords:
Transmission X-ray microscopy
3D μ-CT
Solder joints
Electromigration
Abnormal Cu depletion

ABSTRACT

Electromigration (EM) in microelectronic solder joints was investigated via transmission X-ray microscopy (TXM) in conjunction with three-dimensional computed microtomography (3D μ-CT). This nondestructive analysis provided visualization of the EM dynamics in the encapsulated solder joints and showed the linear dependence of the Cu pad depletion on the current stressing time. Quantitative analysis of the interstitial Cu diffusion in β-Sn based on Huntington's EM theory offered rationalization of this EM-induced degradation mechanism.

Electromigration (EM), mass transport driven by the electron wind force resulting from momentum transfer between electrons and thermally activated atoms due to the scattering effect [1], has become one of the principal factors limiting solder joint performance in microelectronic packaging [2]. Classical EM degradation mechanisms in line-bump solder joints primarily include pancake-like void formation [2–7] and excessive pad depletion [2,8–9]. These degradations are usually initiated at the entrance of the electron flow of a solder bump, quickly spread along the cathode interface, and ultimately cause the overall joint integrity to fail. Because these EM-induced degradations are time-dependent problems, a time-resolved study of the microstructure transition in the solder joints is required to gain a better understanding of the EM mechanisms controlling the joint failure modes. The voiding dynamics in current-stressed solder joints were recently examined via in-/ex-situ X-ray inspections [10–12], and the Johnson–Mehl–Avrami phase transformation mechanism governing the void's growth behavior was confirmed [11]. Here, we demonstrate for the first time the application of transmission X-ray microscopy (TXM) coupled with three-dimensional computed microtomography (3D μ-CT) to nondestructively track the EM-induced Cu pad's depletion in encapsulated solder joints in *real-time*, which advances understanding of the EM failure mechanisms.

In this study, a TXM facility (type: DAGE 7600NT-100) using point projection of the broadband bremsstrahlung radiation (tungsten target) with a spatial resolution of approximately 100 nm was employed to visualize the interior of solder joints under electron current stressing. This TXM analysis, based on the different absorptions of X-ray radiation by different materials, enables a nondestructive, real-time characterization with atomic (Z) discrimination. The solder joints were fabricated via a typical soldering process and had a Cu/solder/Cu structure with a line-bump configuration, as shown in Fig. 1(a). The Cu pads had an opening diameter of 235 μm with a thickness of 25 μm, and the solder bump was made of a Sn-based alloy with a diameter of 200 μm prior to the soldering reaction. Upon current stressing, a 4.4-amp direct current was applied to the joint structure, producing a current density of 1.1×10^4 A/cm^2 (on average) at the Cu/solder contact window and a temperature rise to approximately 160 °C due to Joule heating. With the TXM analysis, the current-stressing test was not interrupted, and mass migration in an encapsulated solder joint can be directly captured, avoiding interruptive/artificial influences that might over-shadow the true EM picture.

Fig. 1(a)–(f) shows a series of snapshots taken by TXM demonstrating the microstructure transition of a Cu/Sn/Cu solder joint under current stressing for the time periods (t): (a) 0 h (initial), (b) 2 h, (c) 4 h, (d) 8 h, (e) 13 h, and (f) 16 h. The Sn-based solder ($Z \approx 50$) absorbed more X-rays (i.e., less X-rays pass through to the detector) than the Cu pad ($Z = 29$) and exhibited darker gray levels in the gray-scale X-ray projections; therefore, the depleted/residue Cu thickness was detectable. Before current stressing (i.e., $t = 0$ h), an equivalent, sunken region at the upper and lower Cu pads is observable in Fig. 1(a), suggesting that a symmetric depletion in Cu occurred in the joint fabrication process. The Cu depletion at this stage resulted from the pad's dissolution into the molten solder and Cu–Sn intermetallic compound (IMC) growth at the interface [13].

* Corresponding author.
E-mail address: ceho1975@hotmail.com (C.-E. Ho).

http://dx.doi.org/10.1016/j.scriptamat.2015.12.001

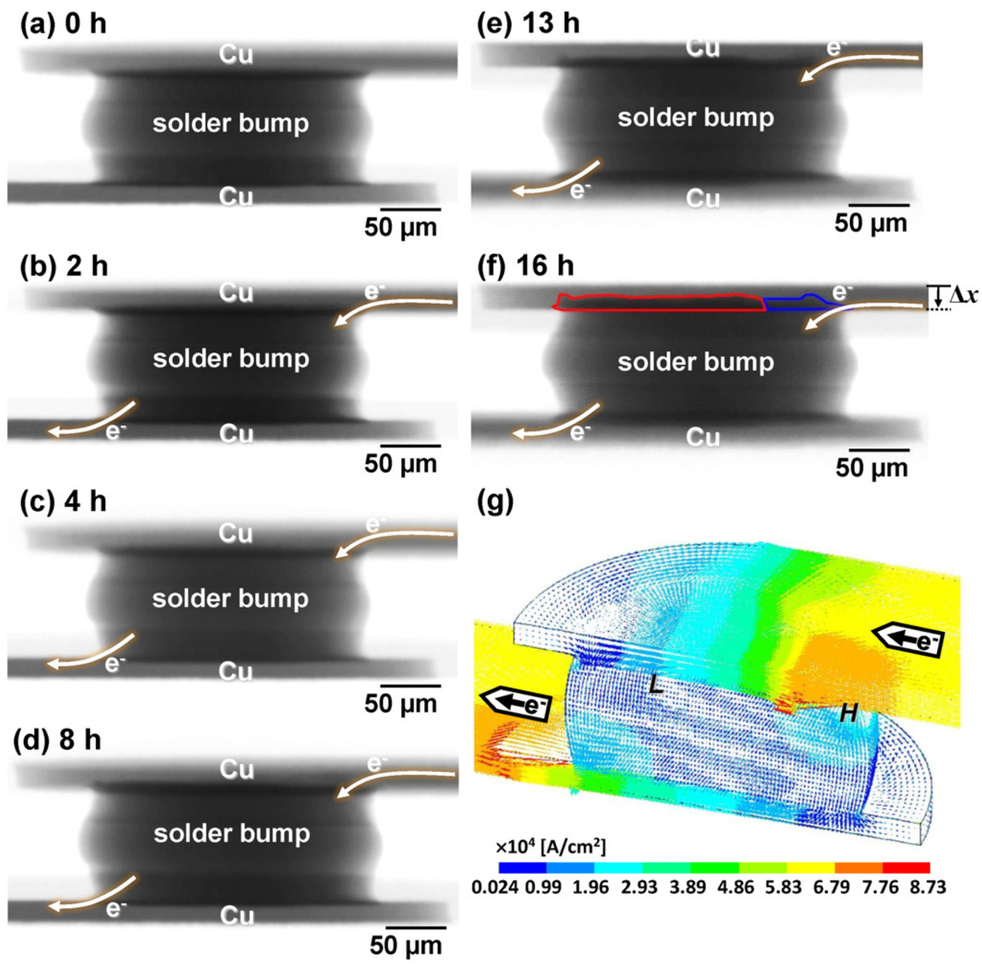

Fig. 1. A series of X-ray micrographs demonstrating the interior microstructure evolution of a solder joint under 1.1×10^4 A/cm^2 current stressing for t = (a) 0 h (initial), (b) 2 h, (c) 4 h, (d) 8 h, (e) 13 h, and (f) 16 h. (g) FEA simulation of the current density distribution with the electron current direction for the solder joint under electron current stressing of 1.1×10^4 A/cm^2 (average).

Upon current stressing, the electron flow enters the solder bump from the upper-right corner and exits from the lower-left corner, as depicted by the arrows of e^- in Fig. 1(b)–(f). Fig. 1(g) shows the current density distribution in the solder joint, which was simulated through ANSYS finite element analysis (FEA) software using the thermal-electric coupled-field element (SOLID69) with a 5-μm mesh size. The vector at the center of each element displays the direction and magnitude of the current stress. The current crowding effect is obvious near the entrance point of the solder bump, pushing the current density in the solder region as high as 3.58×10^4 A/cm^2 (point H, Fig. 1g), even though the global mean current density at the cathode interface is only 1.1×10^4 A/cm^2. The current density value gradually decreases away from the current crowding region (CCR) and becomes approximately one-fifth of the maximum value (i.e., ~7.49×10^3 A/cm^2) at L (solder region). Current stressing caused further Cu depletion, especially for the cathode side, as evidenced by the X-ray micrographs (Fig. 1b–f). Typical EM voids, as observed in Refs. [10–12], did not form at the space of the depleted Cu zone, but the replacement by some materials with a larger Z than Cu did occur. The back-fill Sn to the space due to the Sn concentration gradient between the solder and the Cu depletion zone, as proposed by Liu et al. [14], is a possible explanation of this microstructure transition. The Cu pad gradually depleted as a function of t, with asymmetric depletion according to the location; specifically, significant depletion occurred at L in contrast to H (Fig. 1b–f). Because the upper-right corner neighbors CCR and the upper-left corner distributed with a relatively low current density (Fig. 1g), the observation of the heavy Cu depletion in the upper-left corner (Fig. 1b–f) is in conflict with most of the findings in the literature [2,8–9], where an extremely fast Cu depletion was usually induced at the CCR as a result of the high current stress.

To identify the TXM investigation of the Cu depletion and the unusual EM scenario observed in Fig. 1(b)–(f), μ-CT was used to construct a volumetric (3D) model of the entire solder joint for further characterization of the pad depletion after the stressing test. In the CT scan, the solder joint was rotated through 360 degrees, and a set of X-ray projections was acquired at a 0.5-degree increment to render 3D μ-CT images through professional CT software (i-View 3D, TeraRecon Inc., USA). Fig. 2 displays the virtual slices (cross sections) of the CT volumetric model for the current-stressed joint shown in Fig. 1(f) at $\Delta x = 8$ μm (a), 10 μm (b), and 12 μm (c). The symbol Δx represents the removal of a specific Cu thickness from the cathode side of the CT volumetric model, as schematically illustrated in Fig. 1(f). An irregular, dark region appeared at the upper-left corner of the Cu pad at $\Delta x = 8$ μm (Fig. 2a), corresponding to the heavy Cu depletion zone observed in the X-ray projection (Fig. 1f). This depletion zone propagated to the CCR (Fig. 2b) as Δx increased to 10 μm, suggesting that an additional 2 μm of Cu had been depleted at L in contrast to H. A further increase of Δx to 12 μm would cause the depletion to spread to approximately the entire pad. This result confirms the TXM characterization and shows that a substantial depletion of Cu did occur at the low-current-density distribution region (i.e., L, Fig. 1g), rather than at the entrance of the electron flow (i.e., H, Fig. 1g), where the current crowding effect occurred. The time-resolved, nondestructive analysis of TXM combined with μ-CT provided visualization of the pad's depletion dynamics in the current-